Eur. Phys. J. A (2013) **49**: 31
DOI 10.1140/epja/i2013-13031-x

THE EUROPEAN PHYSICAL JOURNAL A

Regular Article – Theoretical Physics

The electric dipole moment of the deuteron from the QCD θ-term

J. Bsaisou[1,a], C. Hanhart[1,2,3], S. Liebig[1], U.-G. Meißner[1,2,3,4,5], A. Nogga[1,2,3], and A. Wirzba[1,2,3]

[1] Institut für Kernphysik and Jülich Center for Hadron Physics, Forschungszentrum Jülich, D-52425 Jülich, Germany
[2] Institute for Advanced Simulation, Forschungszentrum Jülich, D-52425 Jülich, Germany
[3] JARA – Forces And Matter Experiments, Forschungszentrum Jülich, D-52425 Jülich, Germany
[4] Helmholtz-Institut für Strahlen- und Kernphysik, Universität Bonn, D-53115 Bonn, Germany
[5] Bethe Center for Theoretical Physics, Universität Bonn, D-53115 Bonn, Germany

Received: 10 January 2013 / Revised: 31 January 2013
Published online: 8 March 2013 –
Communicated by M.C. Birse

Abstract. The two-nucleon contributions to the electric dipole moment (EDM) of the deuteron, induced by the QCD θ-term, are calculated in the framework of effective field theory up-to-and-including next-to-next-to-leading order. In particular we find for the difference of the deuteron EDM and the sum of proton and neutron EDM induced by the QCD θ-term a value of $(-5.4 \pm 3.9)\,\bar{\theta} \times 10^{-4}\,e\,\mathrm{fm}$. The by far dominant uncertainty comes from the CP- and isospin-violating πNN coupling constant.

1 Introduction

Under the assumption that the CPT theorem is valid, permanent electric dipole moments (EDMs) of elementary particles and nuclei, which arise under parity P *and* time reflection T breaking, belong to the most promising signals of CP-violating physics beyond the Cabibbo-Kobayashi-Maskawa (CKM) phase of the Standard Model (SM) [1–3]. Possible mechanisms [4, 5] are the dimension-four θ vacuum angle term of Quantum Chromodynamics (QCD) [6] and the effective dimension-six quark, quark-color, and gluon-color terms [7–9] (including certain combinations of four-quark terms [10,11]) resulting from extensions of the SM such as supersymmetry [12], many-Higgs scenarios [13] etc. In refs. [14, 15] it was recently pointed out that the same mechanism that drives the potential CP violation beyond the SM in $D \to K^+K^-/\pi^+\pi^-$ [16, 17] should, if present, also lead to an enhanced nucleon EDM. However, a single successful measurement of an EDM signal of the neutron, say, would not suffice to isolate the specific CP-violating mechanism. Therefore, more than one EDM measurement involving other hadrons and (light) nuclei, *e.g.* the proton, deuteron, helium-3, are necessary in order to uncover the source(s) of the CP breaking.

In recent years various theoretical studies focussed on the calculation of EDMs for light nuclei [18–25], largely triggered by on-going plans for dedicated experiments to measure EDMs of light ions using storage rings [26–30]. These calculations revealed that different CP-violating mechanisms contribute to different probes with different strength. Therefore, non-zero measurements as well as controlled calculations of nucleon and nuclear EDMs are necessary to reveal additional information on the physics beyond the SM that drive non-vanishing EDMs.

In this work we calculate the two-nucleon contribution to the deuteron EDM that would be produced from a non-vanishing QCD θ-term up to next-to-next-to-leading order. Thus, once the EDMs of the proton, neutron and deuteron were measured, the results of our calculation would allow one to extract the value of $\bar{\theta}$ directly from data, assuming that no other CP-violating mechanisms contribute significantly. Since lattice QCD will eventually be able to calculate the neutron and proton EDMs with $\bar{\theta}$ as the only input, a combination of the calculation presented here with lattice QCD and experimental numbers will enable one to decide, if the θ-term is the culprit of generating the EDMs. Note that direct lattice calculations for nuclear EDMs would be much more challenging.

The terms of the CP-violating interaction Lagrangian relevant for this work are given by —see ref. [23] and references therein—

$$\begin{aligned}\mathcal{L}_{\not{CP}} = {} & \bar{N}\left(b_0 + b_1\tau_3\right) S^\mu N v^\nu F_{\mu\nu} + g_0 \bar{N}\boldsymbol{\pi}\cdot\boldsymbol{\tau}N + g_1 \bar{N}\pi_3 N \\ & + C_1^0 \bar{N}ND_\mu(\bar{N}S^\mu N) + C_2^0 \bar{N}\boldsymbol{\tau}ND_\mu(\bar{N}\boldsymbol{\tau}S^\mu N) \\ & + C_1^3 \bar{N}\tau_3 ND_\mu(\bar{N}S^\mu N) + C_2^3 \bar{N}ND_\mu(\bar{N}\tau_3 S^\mu N) \\ & + \ldots . \end{aligned} \tag{1}$$

Here $v^\mu = (1, \mathbf{0})$, $S^\mu = (0, \frac{1}{2}\boldsymbol{\sigma})$ and $\boldsymbol{\tau}$ are the nucleon velocity, spin and isospin, respectively, while D_μ

[a] e-mail: j.bsaisou@fz-juelich.de

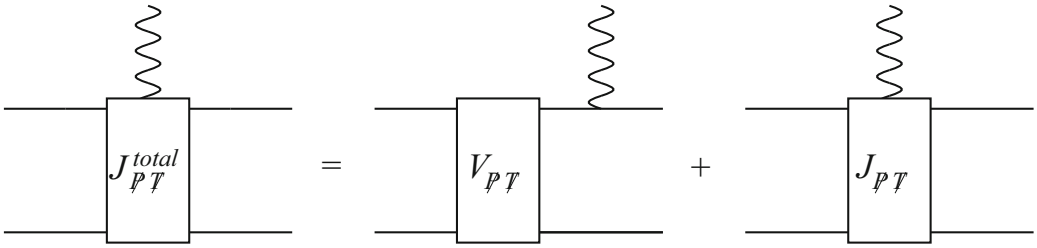

Fig. 1. Total CP-violating transition current. The P and T violation stem from either CP-violating two-nucleon potentials or two-nucleon–irreducible CP-violating transition currents.

is the covariant derivative. For θ-term–induced CP violation naive dimensional analysis (NDA) gives that $g_1^\theta/g_0^\theta \sim \epsilon M_\pi^2/m_N^2$ [31]. However, as already pointed out in ref. [19] and refined further below, g_1^θ is significantly enhanced compared to this estimate —in fact, the contribution from g_1^θ dominates the deuteron EDM.

The single-nucleon EDM from the θ-term starts to contribute at the one-loop level [4, 5]. At the same order there are two counterterms, proportional to b_0 and b_1, to absorb the divergence [32–34] —a proof that only two low-energy constants appear in three-flavor chiral perturbation theory at next-to-leading order was recently given in ref. [35]. Therefore, although the value of the CP-violating coupling constants g_0 and g_1 can be related to the strength of the QCD θ-term, $\bar\theta$, within the effective field theory the same is not possible for the EDM of a *single* neutron or proton. This is different in case of the nuclear EDMs: for the *few-nucleon* contributions, counterterms appear only at subleading orders and therefore controlled calculations become feasible, although, in case of the deuteron EDM, with a sizable uncertainty. Such subleading terms can be found in the second and third lines of eq. (1), where the two terms in the third line are additionally suppressed by isospin breaking. The dots in eq. (1) denote further CP-violating terms that do not contribute to the deuteron EDM at orders considered in this work. These terms include CP-violating $NN\pi\gamma$-, $NN\pi\pi$-, $NN\pi\pi\gamma$-, $4N\gamma$-terms, CP-violating photon–two-pion terms, and CP-violating pure pion terms (see ref. [31] for the latter class).

There are two types of contributions that are relevant for the present study, namely CP-violating NN interactions and CP-violating irreducible $NN \to NN\gamma$ transition currents —cf. fig. 1. As will be outlined below, for the deuteron EDM the latter kind of contributions contains at its leading non–vanishing order loop diagrams that are calculated in this work for the first time.

The paper is structured as follows: in sect. 2 the prefactors of the CP-violating πNN couplings g_0^θ and g_1^θ are derived from the QCD θ-term. After this, a brief discussion of the power counting is presented in sect. 3. Section 4 contains the derivation of the two-nucleon contributions to the deuteron EDM induced by the θ-term, where the NN potential and transition current contributions are discussed in subsects. 4.1 and 4.2, respectively. Finally, in sect. 5 a short summary of the presented results and an outlook are given. The role that the vacuum alignment plays for the generation of g_1^θ is outlined in appendix A. Appendices B and C present two further alternatives to derive the CP-violating coupling constant g_1^θ, an update of the original derivation by Lebedev *et al.* [19] and a derivation in the framework of $SU(3)$ chiral perturbation theory (ChPT), similarly to the one of g_0^θ by [5, 32–34], respectively. Finally, appendix D is reserved for an estimate of the g_1^θ contribution resulting from a resonance saturation mechanism involving the odd-parity nucleon-resonance $S_{11}(1535)$.

2 CP-violating πNN couplings from the θ-term

On the quark level the effect of the θ-term can be written as $m_*\bar\theta\bar q i\gamma_5 q$ [5], with the reduced quark mass $m_* \equiv m_u m_d/(m_u+m_d) = (m_u+m_d)(1-\epsilon^2)/4$, where $\epsilon = (m_u-m_d)/(m_u+m_d) = -0.35 \pm 0.10$ [36]. It thus behaves under chiral rotations identically to the quark mass term and can be included in the chiral Lagrangian via

$$\chi_\pm = u^\dagger \chi u^\dagger \pm u \chi^\dagger u \quad \text{with} \quad \chi = 2B(s+ip), \tag{2}$$

where s may for our purposes be identified with the quark mass matrix, which reads

$$\mathcal{M} = \frac{m_u+m_d}{2}\,\mathbf{1}_2 + \frac{m_u-m_d}{2}\tau_3, \tag{3}$$

while $p = m_*\bar\theta\,\mathbf{1}_2$. The pion fields are contained in the usual $SU(2)$ matrix $u = U^{1/2}$, see, *e.g.*, [37].

Starting point for the calculation of the CP-violating πNN vertices are, to the order we are working, the quark-mass–dependent terms of the CP-conserving Lagrangian $\mathcal{L}^{(2)}_{\pi N}$ [37], namely

$$\begin{aligned} &c_1\, N^\dagger \langle \chi_+ \rangle N + c_5 N^\dagger \left[\chi_+ - \frac{1}{2}\langle\chi_+\rangle\right] N = \\ &c_1\, 4B(m_u+m_d) N^\dagger N \\ &+ c_5\, 2B\, N^\dagger \left[(m_u-m_d)\tau_3 + \frac{2m_*\bar\theta}{F_\pi}(\boldsymbol{\pi}\cdot\boldsymbol{\tau})\right] N \\ &+ \dots\,. \end{aligned} \tag{4}$$

Here $\langle\cdot\rangle$ denotes the trace in flavor space. The dots indicate that terms not relevant for this study were omitted.

We start with a discussion of the term proportional to c_5. The first term of the third line of eq. (4) leads to the quark-mass-induced part of the proton-neutron mass difference, $\delta m_{np}^{\rm str}$. It can be quantified from three different sources: i) the use of dispersion theory to quantify the electromagnetic part of the proton-neutron mass difference [38–41], ii) lattice QCD [42], or iii) from charge-symmetry-breaking (CSB) studies of $pn \to d\pi^0$ [43]. All analyses lead to consistent results, with the first one being the most accurate. Thus we will use [41]

$$4B(m_u - m_d)c_5 = \delta m_{np}^{\rm str} = (2.6 \pm 0.5)\,\text{MeV}. \quad (5)$$

From this we get

$$g_0^\theta = \frac{\delta m_{np}^{\rm str}(1-\epsilon^2)}{4F_\pi \epsilon}\,\bar\theta = (-0.018 \pm 0.007)\,\bar\theta, \quad (6)$$

for the prefactor of the second term of the third line of eq. (4), which is of isospin-conserving nature —cf. eq. (1). Here we used $F_\pi = 92.2\,\text{MeV}$ [36]. The superscript θ indicates that we here only include the strength that comes from the θ-term. The expression given above agrees with the prediction of ref. [44] when eq. (14) of ref. [44] is inserted into the corresponding eq. (8)[1]. It turns out that the value of g_0^θ is more than a factor of 10 smaller than the estimate from NDA given by $\bar\theta M_\pi^2/(m_N F_\pi)$ in terms of the pion mass M_π, the nucleon mass m_N and the pion axial decay constant F_π.

The first term in the second line of eq. (4) leads to the quark-mass–induced isoscalar contribution to the nucleon mass —thus c_1 can be related to the πN sigma term. For this low-energy constant (LEC) we use the value given in ref. [45],

$$c_1 = (-1.0 \pm 0.3)\,\text{GeV}^{-1}, \quad (7)$$

which is a compilation of various extractions of c_1 [46–49]. At this stage this contribution does not contain a CP-odd term, however, as outlined in ref. [31] and detailed within our formalism in appendix A, in the presence of CP violation a rotation of the vacuum is necessary in order to remove pion tadpoles from the theory. This rotation induces an additional CP-violating term in the pion-nucleon sector; namely, in agreement with ref. [31] we find a coupling of g_1 type,

$$g_1^\theta = \frac{2\,c_1\,(\delta M_\pi^2)^{\rm str}\,(1-\epsilon^2)}{F_\pi\,\epsilon}\bar\theta, \quad (8)$$

where $(\delta M_\pi^2)^{\rm str}$ denotes the quark-mass–induced part of the mass square splitting between charged and neutral pions. Moreover, the above-mentioned vacuum rotation produces as well a correction to g_0^θ, which, however, is numerically negligible.

Inserting the relation [50]

$$(\delta M_\pi^2)^{\rm str} \approx \frac{B}{4}\frac{(m_u-m_d)^2}{m_s-(m_u+m_d)/2} \approx \frac{\epsilon^2}{4}\frac{M_\pi^4}{M_K^2-M_\pi^2} \quad (9)$$

[1] The result of ref. [44] has the opposite sign to ours (which is compensated by the opposite sign of ϵ). Furthermore, F_π is defined twice as large there.

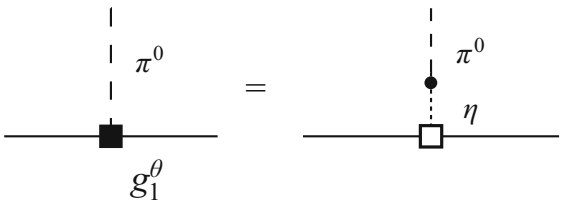

Fig. 2. CP-violating $\pi^0 NN$ vertex g_1^θ (black square) induced by π^0-η mixing and the CP-violating ηNN vertex (open square).

into eq. (8) we get the result

$$g_1^\theta \approx \frac{c_1(1-\epsilon^2)\epsilon}{2F_\pi}\frac{M_\pi^4}{M_K^2-M_\pi^2}\,\bar\theta = (0.003 \pm 0.001)\,\bar\theta, \quad (10)$$

where the uncertainty of this contribution is dominated by the uncertainty in c_1. The expression given in (10) exactly agrees with the one presented in appendix B which is derived from η-π^0 mixing, see ref. [19] and fig. 2, provided the strange-quark content of the nucleon is vanishingly small. An alternative derivation, which uses $SU(3)$ ChPT input instead of sigma-term estimates, is presented in appendix C. Taking the rather large $SU(3)$ errors into consideration, the $SU(3)$ estimates for g_1^θ (and g_0^θ) are compatible with our final values which are quoted at the end of this section.

In addition to the contribution related to the πN sigma term there exists one additional, linearly independent operator structure that leads to a contribution to g_1^θ, see ref. [31]. In our notation, it is given by

$$\frac{c_1^{(3)}}{4} N^\dagger \langle \chi_- \rangle^2 N = c_1^{(3)}\frac{B^2 m^*(m_u-m_d)}{F_\pi}\bar\theta N^\dagger \pi_3 N + \ldots . \quad (11)$$

Unfortunately, this operator structure contributes to CP-conserving observables at such a high order that it cannot be constrained from a study of, say, πN scattering. Thus we need to estimate the value of $c_1^{(3)}$ differently. While the operator χ_+ leads to terms that are even (odd) in the pion field for CP-conserving (violating) contributions, these relations are inverted for the operators χ_-: CP-conserving (violating) contributions are given by terms that are odd (even) in the pion field. Thus, a natural resonance saturation estimate for the operator of eq. (11) is given by a diagram, where one insertion of χ_- converts the even-parity nucleon into the lowest odd-parity nucleon resonance, the $S_{11}(1535)$, which then decays via an isospin-violating decay into a neutral pion and a nucleon. The latter step may be modeled by a $S_{11}(1535)$ decaying into ηN which then converts into $\pi^0 N$ via η-π mixing. This contribution is potentially important, since the coupling of this nucleon resonance to ηN is very significant [36]. However, an explicit calculation, see appendix D, shows that the mentioned contribution does not exceed the value estimated from NDA. Moreover, in order to get the proper $SU(3)$ chiral limit of QCD, the η should be coupled with a derivative even to the nucleon resonances —the resulting Lagrangian

is given in ref. [51]— which leads to an additional suppression. We therefore consider it safe to estimate the additional g_1^θ uncertainty due to our ignorance of $c_1^{(3)}$ from an NDA estimate which is equal to $\epsilon M_\pi^4/(m_N^3 F_\pi) \sim 0.002$. In what follows we will therefore use

$$g_1^\theta = (0.003 \pm 0.002)\bar{\theta}, \tag{12}$$

which includes zero within two sigma. In particular, we find for the ratio

$$\frac{g_1^\theta}{g_0^\theta} = \frac{8c_1(\delta M_\pi^2)^{\rm str}}{\delta m_{np}^{\rm str}} = -0.2 \pm 0.1. \tag{13}$$

The value of g_1^θ/g_0^θ is numerically about a factor of 25 larger than the $SU(2)$ estimate of order $\epsilon M_\pi^2/m_N^2$, which would follow from the first relation of eq. (13) if the scaling $\delta m_{np}^{\rm str} \sim \epsilon M_\pi^2/m_N$ were assumed. The main origin of this difference is that g_0^θ is unusually small —instead of two powers in the counting the relative suppression numerically is of the order of one power in the expansion parameter M_π/m_N. It is this observation that we will use in the power counting as outlined in the next section.

3 Power counting

It is crucial for this study to identify a power counting that allows a comparison of the contributions to the nuclear EDMs from CP-odd transition currents to those from the CP-odd NN potential. The power counting originally proposed by Weinberg for nuclear matrix elements [52], in spite of its many successful applications, is not able to explain analogous ratios studied numerically in ref. [53] —we will therefore modify it slightly, as explained below. An alternative scheme is presented in ref. [23].

In Weinberg's counting, contributions to the deuteron EDM that come from a CP-violating potential (cf. fig. 1) are regarded as reducible, while the transition currents are counted as irreducible. Thus, one needs to power-count the nuclear wave functions and the photon couplings separately, making it necessary to assign a scale to a disconnected nucleon line. For dimensional reasons the corresponding $\delta^{(3)}$ function is identified with $1/p^3$, where p denotes the typical momentum appearing in the evaluation of the integrals, identified with the pion mass, M_π. However, if indeed nucleon momenta are of order M_π, the two-nucleon intermediate state appearing between the photon coupling and the CP-violating NN potential is off-shell. Thus, also this contribution is to be regarded as irreducible with the two-nucleon propagator counted as $(p^2/m_N)^{-1}$, where m_N denotes the nucleon mass. Again p is identified with M_π. This power counting properly explains the numerical observations of ref. [53] and will be used in this work as well. For more details we refer to ref. [54].

3.1 Power counting for the contributions of the single-nucleon EDMs

In a world where CP violation beyond the SM is driven by the θ-term, within the effective field theory the single-nucleon EDMs start at the one-loop level. At the same order there are two counterterms —the b_i terms in eq. (1). The isospin structure of the loops gives that the isoscalar component of the single-nucleon EDMs is suppressed by one order in the counting compared to the isovector one [4,5]. However, this suppression is not present for the counterterms [32,33], and therefore for the power counting we may estimate both the contribution from the d_0 as well as the d_1 term from the estimate for the leading loop contribution given by

$$g_0^\theta \times (M_\pi/F_\pi) \times (eM_\pi) \times (1/M_\pi^5) \times (M_\pi)^4/(4\pi)^2 \sim eg_0^\theta F_\pi M_\pi/m_N^2,$$

where the dimension-full factors in the first line come from the regular πNN vertex, the photon-pion vertex (with the electron charge $e < 0$), the propagators and the integration measure, respectively, and we identified $(4\pi F_\pi) \sim m_N$. In order to derive from this the total transition current we need to multiply the estimate with $(1/F_\pi^2) \times m_N/M_\pi^2$ from the NN potential and the two-nucleon propagator, respectively. We therefore find an estimate of the order of $eg_0^\theta/(F_\pi m_N M_\pi)$ from the single-nucleon EDM for the leading contribution to the total transition current. Thus, the single-nucleon EDMs start to contribute to the deuteron EDM at NLO, as we will outline in the next subsections —cf. table 1.

3.2 Power counting of the irreducible CP-odd NN potential

The leading diagrams for the irreducible CP-odd NN potential are shown in fig. 3. The leading, isospin-conserving, CP-odd one-pion exchange can be estimated as $g_0^\theta/(M_\pi F_\pi)$. However, as will be discussed in the next section, this term does not contribute to the deuteron EDM due to selection rules. The first non-vanishing contribution comes from the subleading, isospin- and CP-odd coupling g_1^θ. It is estimated to contribute as $g_1^\theta/(M_\pi F_\pi) \sim g_0^\theta/(m_N F_\pi)$, where we used the empirical relation, presented in the previous section, $g_1^\theta/g_0^\theta \sim M_\pi/m_N$. This contribution will be called leading order (LO).

A CP-odd pion exchange potential from a g_0^θ coupling on one vertex and an isospin-odd, CP-conserving coupling on the other also leads to a non-vanishing contribution to the deuteron EDM [19,23]. As long as we focus only on contributions to the deuteron EDM, the impact of the resulting potential is effectively a redefinition $g_1^\theta \to g_1^\theta[1 + g_0^\theta \beta_1/(2g_A g_1^\theta)]$ [23], where β_1 is the strength parameter of the isospin-odd, CP-even πNN vertex and g_A is the axial-vector coupling constant of the nucleon. The Nijmegen partial-wave analysis provides $|\beta_1| \leq 10^{-2}$ [55], which is consistent with estimating its value from the same mechanism used in ref. [19] and appendix B, namely via η–π^0 mixing —see fig. 4. Thus the inclusion of β_1 shifts g_1^θ by a few percent at most and can therefore be neglected, given the significant uncertainty of g_1^θ.

Table 1. Power counting scales of the CP-violating NN potentials (left) and (total) transition currents (right) relevant for the two-nucleon contribution to the θ-term–induced EDM of the deuteron, where the equivalence $4\pi F_\pi \sim m_N$ is assumed.

	NN potential			(Total) transition current		
LO	$g_0^\theta/(m_N F_\pi)$	$\sim$	$g_1^\theta/(M_\pi F_\pi)$	$g_0^\theta\, e/(M_\pi^2 F_\pi)$	$\sim$	$g_1^\theta\, e\, m_N/(M_\pi^3 F_\pi)$
NLO	$g_0^\theta M_\pi/(m_N^2 F_\pi)$	$\sim$	$g_1^\theta/(m_N F_\pi)$	$g_0^\theta\, e/(M_\pi m_N F_\pi)$	$\sim$	$g_1^\theta\, e/(M_\pi^2 F_\pi)$
N^{2}LO	$g_0^\theta M_\pi^2/(m_N^3 F_\pi)$	$\sim$	$g_1^\theta M_\pi/(m_N^2 F_\pi)$	$g_0^\theta\, e/(m_N^2 F_\pi)$	$\sim$	$g_1^\theta\, e/(M_\pi m_N F_\pi)$

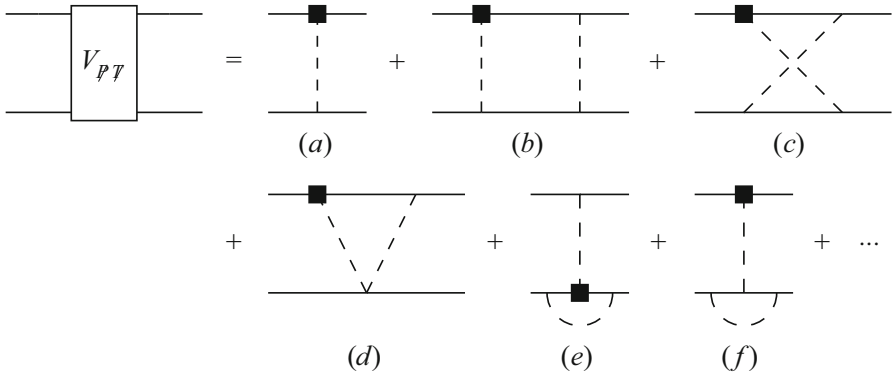

Fig. 3. Contributions to the CP-violating two-nucleon potential: (a) LO contributions, (b)–(f) NLO and N^{2}LO contributions, where the former class contains the g_0^θ and the latter the g_1^θ coupling. Solid lines denote nucleons and dashed lines denote pions. The CP-violating vertex is depicted by a black box. For each class of diagrams only one representative is shown.

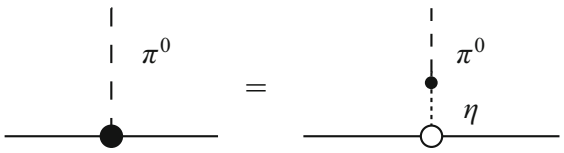

Fig. 4. Isospin-odd CP-conserving πNN vertex (black circle) induced by π^0-η mixing and the CP-conserving ηNN coupling (open circle).

The first relativistic correction is the recoil correction to the g_A vertex, given by $-g_A/(2m_N F_\pi) S\cdot(p_1+p_2) v\cdot k \tau^a$ where $p_{1,2}$ are the nucleon momenta and k is the outgoing pion momentum. The corresponding contribution is suppressed by three orders relative to the one of the g_A vertex due to the additional energy dependence (since $v = (1, \mathbf{0})$ and $k = p_1 - p_2$).

To one-loop order there are a couple of diagrams as shown in fig. 3. The power counting gives for these diagrams $g_0^\theta M_\pi/(m_N^2 F_\pi)$, where we identified $4\pi F_\pi \sim m_N$. Thus, the loop contributions with the CP violation induced via the coupling g_0^θ are suppressed relative to the leading, non-vanishing contribution to the potential (proportional to g_1^θ) by one power of M_π/m_N and therefore contribute to NLO. However, as outlined below, the spin-isospin structure of all these diagrams is such that they do not contribute to the deuteron EDM. At N^{2}LO the same topologies appear, however, with g_0^θ replaced by g_1^θ. In addition, also triangle topologies of type (d) with the $\pi\pi NN$ vertex from $\mathcal{L}_{\pi N}^{(2)}$ [37] as well as vertex corrections (diagrams (e) and (f)) formally appear at this order. As shown below, besides the latter class none of the mentioned diagrams contributes to the deuteron EDM.

On dimensional grounds CP-odd four-nucleon operators start to contribute at order M_π/m_N relative to the leading term. Their largest θ-term–induced contributions are isospin conserving (cf. second line of eq. (1)). Thus, as a consequence of the Pauli Principle, they change the two-nucleon spin. Therefore they do not contribute to the deuteron EDM. However, their isospin-violating counterparts (cf. third line of eq. (1)) contribute, but have a relative suppression of order $(M_\pi/m_N)^2$ and are therefore of N^{3}LO.

In summary, to the order we are working, the only contribution to the CP-odd NN potential that needs to be considered for the deuteron EDM is the isospin-odd tree-level contribution proportional to g_1^θ and its vertex corrections.

3.3 Power counting of the irreducible transition currents

We now turn to the transition currents. As explained in the beginning of this section, in order to compare the contribution from the CP-odd NN potential to that of the CP-odd transition currents, the former needs to be multiplied by $e\, m_N/M_\pi^2$. Thus, the *leading-order contribution* of the total transition current is estimated to scale as $g_1^\theta\, e\, m_N/(M_\pi^3 F_\pi) \sim g_0^\theta\, e/(M_\pi^2 F_\pi)$.

The tree-level contribution, shown in fig. 5, is formally of NLO, however, turns out to be of isovector character and thus does not add to the deuteron EDM.

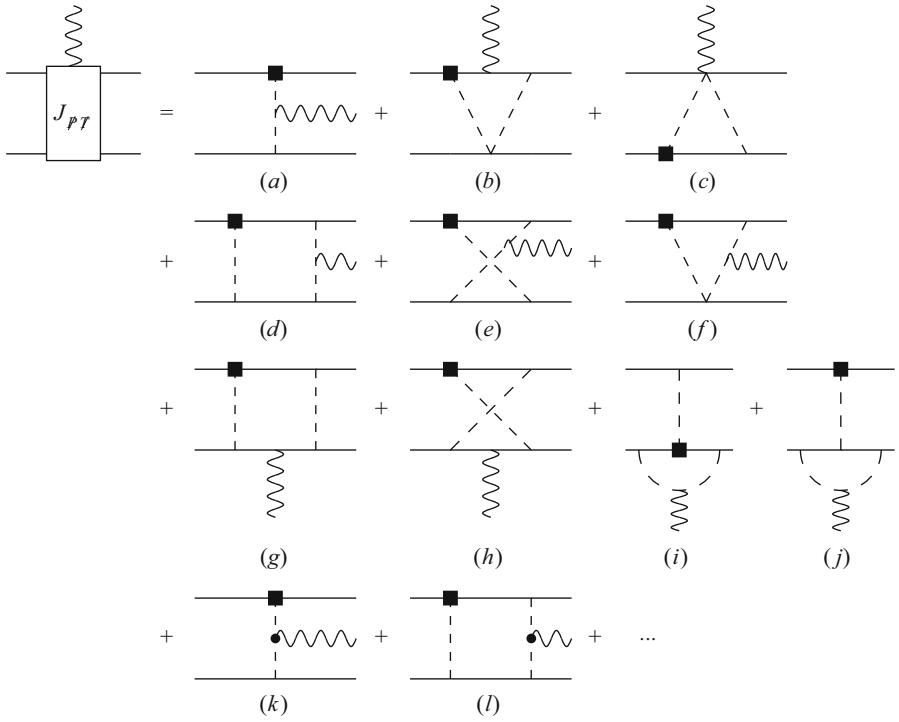

Fig. 5. Contributions to the CP-violating transition current: (a) NLO contribution, (b)–(l) N^{2}LO contributions. Solid lines denote nucleons and dashed line denote pions. The CP-violating vertex is depicted by a black box, a CP-conserving, but isospin-violating vertex by a filled circle. For each class of diagrams only one representative is shown.

The one-loop contributions to the irreducible transition current are estimated as $g_0^\theta\, e/(m_N^2 F_\pi)$ and are therefore of N^{2}LO. The naive power counting of the diagram classes depicted in fig. 5 (d) and fig. 5 (e) is slightly more subtle due to the cancellation of one of the nucleon propagators by the energy dependence of the $\pi\pi\gamma$ vertex. Therefore these diagrams are part of the irreducible transition current and appear at N^{2}LO.

Finally there are two additional structures —fig. 5 (k) and (l)— that appear since the zeroth component of the $\gamma\pi\pi$ vertex is proportional to the energy exchanged and thus gets sensitive to the total neutron-proton mass difference[2], δm_{np}. The contributions of the diagrams of fig. 5 (k) and (l) can be estimated as $g_0^\theta e\delta m_{np}/(M_\pi^3 F_\pi)$ and $g_0^\theta e\delta m_{np}/(m_N M_\pi^2 F_\pi)$, respectively. Thus the former (latter) appears to be suppressed by $\delta m_{np}/M_\pi$ $(\delta m_{np}/m_N)$ compared to the leading order. Based on NDA one might assign $\delta m_{np} \sim \epsilon M_\pi^2/m_N$ such that diagram (k) would appear at NLO, while diagram (l) would appear at N^{2}LO. However, as argued above, the nucleon mass difference is significantly smaller than its NDA estimate —this observation made us assign $g_1^\theta/g_0^\theta \sim M_\pi/m_N$, and not $(M_\pi/m_N)^2$ as would follow from NDA. In full analogy we now assign diagram (k) and diagram (l) the orders N^{2}LO and N^{3}LO, respectively. Therefore the former is included in our calculation while the latter can be neglected.

In table 1 the power counting scales of the CP-violating irreducible NN potentials and those of the irreducible as well as of the total transition currents can be found. This completes the discussion of the power counting. In the next section the various diagrams are discussed explicitly.

4 EDMs from the θ-term

The computation of the two-nucleon contributions to the deuteron EDM is most efficiently performed in the Breit frame defined by $q = P - P' = (0, \boldsymbol{P} - \boldsymbol{P'})$ where P and P' denote the total four-momenta of the incoming and outgoing deuteron states and q the momentum of the external "Coulomb-like" photon. The electric dipole moment d of the deuteron nucleus of mass m_D is then defined (in analogy to the magnetic moment case) by

$$d = \lim_{\boldsymbol{q}\to 0} \frac{F_3(\boldsymbol{q}^2)}{2m_D}\,, \tag{14}$$

where the electric dipole form factor F_3 is related to the P- and T-violating transition current operator $(J^{\rm total}_{\not P \not T})^\mu$ by

$$\left\langle J=1, J_z'=\pm 1; \boldsymbol{P'} \left| (J^{\rm total}_{\not P \not T})^0 \right| J=1, J_z=\pm 1; \boldsymbol{P} \right\rangle = \mp i q^3 \frac{F_3(\boldsymbol{q}^2)}{2m_D}\,, \tag{15}$$

where J is the total angular momentum of the deuteron and J_z and J_z' its z-components for the in- and out-state, respectively.

[2] We would like to thank J. de Vries, U. van Kolck and R.G.E. Timmermans for drawing our attention to these currents. The same effect in a different context is discussed in detail in ref. [43].

Table 2. Leading-order contributions to the deuteron EDM from the g_1^θ vertex without (d_{PW}^θ, PW: plane wave) and with (d_{MS}^θ, MS: multiple scattering) intermediate $^3P_1$-interactions and the total leading-order contribution d_{LO}^θ in units of $(g_1^\theta/g_0^\theta)G_\pi^0\, e\,\mathrm{fm}$ with $G_\pi^0 = g_0^\theta g_A m_N/F_\pi$ – calculated in Zero-Range Approximation (ZRA), with the Argonne v_{18} [61], Reid93 [62] and CD-Bonn [56] potentials.

	Potential	$^3D_1$-admixture	d_{PW}^θ	d_{MS}^θ	d_{LO}^θ
[18,22]	ZRA	–	$-1.8\cdot10^{-2}$	–	$-1.8\cdot10^{-2}$
[20,63]	A v_{18}	5.76%			$-1.43\cdot10^{-2}$
[20,63]	Reid93	5.7%			$-1.45\cdot10^{-2}$
[24,25]	Reid93	5.7%	$-1.93\cdot10^{-2}$	$0.40\cdot10^{-2}$	$-1.53\cdot10^{-2}$
This work	CD-Bonn	4.8%	$-1.95\cdot10^{-2}$	$0.44\cdot10^{-2}$	$-1.52\cdot10^{-2}$

The total CP-violating transition current $J_{\not P\not T}^{\text{total}}$ can be separated into two contributions of different topology (see fig. 1): two-nucleon–reducible transition currents where the P and T violation is induced by a CP-violating two-nucleon potential on the one hand, and irreducible CP-violating transition currents on the other. These will now be discussed in detail.

4.1 Contributions from the CP-odd NN potential to the deuteron EDM

In order for a P- and T-violating two-nucleon potential to contribute in the deuteron channel, it must induce $^3S_1$-$^3D_1 \to {}^3P_1$ transitions, *i.e.* isospin-0 to isospin-1 and spin-1 to spin-1 transitions since the photon-nucleon coupling is spin independent —it therefore must be antisymmetric in isospin space and symmetric in spin space.

Contributions to the CP-violating two-nucleon potential can be further separated into irreducible and reducible potentials. The latter class consists of a CP-violating potential and of multiple insertions of the NN potential in the $^3S_1$-$^3D_1$ state and/or in the intermediate $^3P_1$ state, which can be either absorbed into the deuteron wave functions, or into the intermediate NN interactions in the $^3P_1$ state and therefore do not need to be considered separately.

The leading contribution to the CP-violating two-nucleon potential is the class of tree-level diagrams depicted in fig. 3 (*a*). The tree-level potential induced by the g_0^θ vertex is given by [10,18]

$$V_{3(a)}(\boldsymbol{l}) = i\frac{g_0^\theta g_A}{2F_\pi}\frac{\boldsymbol{l}}{\boldsymbol{l}^2+M_\pi^2}\cdot(\boldsymbol{\sigma}_{(1)}-\boldsymbol{\sigma}_{(2)})\,\boldsymbol{\tau}_{(1)}\cdot\boldsymbol{\tau}_{(2)}, \qquad (16)$$

where $\boldsymbol{l}$ denotes the pion momentum running from nucleon 1 to nucleon 2. It is spin antisymmetric and isospin symmetric and does not induce $^3S_1$-$^3D_1 \to {}^3P_1$ transitions [10,18,20].

The potential induced by the g_1^θ vertex reads

$$V_{3(a)}^{\theta\,\mathsf{LO}}(\boldsymbol{l}) = i\frac{g_1^\theta g_A}{4F_\pi}\frac{\boldsymbol{l}}{\boldsymbol{l}^2+M_\pi^2}\cdot\Big[(\boldsymbol{\sigma}_{(1)}+\boldsymbol{\sigma}_{(2)})(\tau_{(1)}^3-\tau_{(2)}^3) + (\boldsymbol{\sigma}_{(1)}-\boldsymbol{\sigma}_{(2)})(\tau_{(1)}^3+\tau_{(2)}^3)\Big], \qquad (17)$$

with $\boldsymbol{l}$ as above. It is the same as in [10, 18, 20] with g_1^θ replaced by g_1. This potential operator has a spin-symmetric and isospin-antisymmetric component and thus contributes to the transition current in the deuteron channel. In order to evaluate its contribution to the EDM of the deuteron we resort to the parametrization of the deuteron wave function of [56] with a $^3D_1$-state probability of 4.8%. In order to include the NN interactions in the intermediate $^3P_1$-state we use the separable rank-2 representation of the Paris nucleon-nucleon potential of ref. [57] (PEST). The resulting contributions to the deuteron EDM listed in table 2 are in agreement with the results for g_1 of ref. [20] using the Argonne v_{18} potential, of refs. [20,24,25] using the Reid93 potential, and of refs. [18,22], where the deuteron wave function has been used in the Zero-Range Approximation (ZRA). The $^3D_1$-admixture is found to enhance the deuteron EDM by about 20%, whereas the interaction in the intermediate $^3P_1$-state reduces the contribution by about the same amount.

Loops formally start to contribute at NLO. The reducible component of the box potential of fig. 3 (*b*) constitutes a static one-pion exchange and is already accounted for either by the deuteron wave functions or by the interaction in the intermediate $^3P_1$-state. Its irreducible component may be obtained by shifting the pole of one of the nucleon propagators into the half plane of the pole of the other nucleon propagator, as outlined in [58–60]: $i/(-v\cdot p_i+i\epsilon) \to -i/(v\cdot p_i+i\epsilon)$. For the sum of the irreducible part of the box potential of fig. 3 (*b*) and the crossed-box potential of fig. 3 (*c*), one finds in dimensional regularization in d space-time dimensions

$$V_{3(b+c)}^{\theta\,\mathsf{NLO}}(\boldsymbol{l}) = -i\frac{g_0^\theta g_A^3}{16\pi^2F_\pi^3}\frac{1+\frac{3}{2}\xi}{\sqrt{\xi(1+\xi)}}\ln\left(\frac{\sqrt{1+\xi}+\sqrt{\xi}}{\sqrt{1+\xi}-\sqrt{\xi}}\right) \times\boldsymbol{\tau}_{(1)}\cdot\boldsymbol{\tau}_{(2)}(\boldsymbol{\sigma}_{(1)}-\boldsymbol{\sigma}_{(2)})\cdot\boldsymbol{l}, \qquad (18)$$

with $\xi = \boldsymbol{l}^2/(4M_\pi^2)$. The divergence has been absorbed by a redefinition of the four-nucleon coupling constant C_2^0 (the scale μ is introduced in dimensional regularization)

$$C_2^0 \to C_2^0 - \frac{g_0^\theta g_A^3}{F_\pi^3}\left[6L - \frac{3}{16\pi^2}\left(\ln\left(\frac{\mu^2}{M_\pi^2}\right)-1\right) - \frac{2}{16\pi^2}\right], \qquad (19)$$

with

$$L = \frac{\mu^{d-4}}{16\pi^2}\left\{\frac{1}{d-4}+\frac{1}{2}\big[\gamma_E-1-\ln(4\pi)\big]\right\}, \qquad (20)$$

where $\gamma_E = 0.577215\ldots$ is the Euler-Mascheroni constant.

The triangular potential of fig. 3 (*d*) gives

$$V^{\theta\,\mathsf{NLO}}_{3(d)}(\boldsymbol{l}) = i\frac{g_0^\theta g_A}{32\pi^2 F_\pi^3}\sqrt{\frac{1+\xi}{\xi}}\ln\left(\frac{\sqrt{1+\xi}+\sqrt{\xi}}{\sqrt{1+\xi}-\sqrt{\xi}}\right) \times \boldsymbol{\tau}_{(1)}\cdot\boldsymbol{\tau}_{(2)}(\boldsymbol{\sigma}_{(1)}-\boldsymbol{\sigma}_{(2)})\cdot\boldsymbol{l}, \quad (21)$$

where the divergence has been absorbed by a further redefinition of C_2^0,

$$C_2^0 \to C_2^0 - \frac{g_0^\theta g_A}{F_\pi^3}\left[-2L+\frac{1}{16\pi^2}\left(\ln\left(\frac{\mu^2}{M_\pi^2}\right)-1\right)+\frac{2}{16\pi^2}\right]. \quad (22)$$

These results reproduce those of ref. [10]. Note that all g_0^θ potential operators up to one loop as well as the four-nucleon-vertex operators are isospin symmetric and spin antisymmetric and therefore vanish in the deuteron channel.

At $\mathsf{N^2LO}$ there are the same topologies as just discussed, however, with the g_0^θ vertex replaced by its isospin-violating counterpart g_1^θ. The triangular-potential operator fig. 3 (*d*) vanishes at the considered order. The class of the crossed-box-potential diagrams of fig. 3 (*c*) gives

$$V^{\theta\,\mathsf{N^2LO}}_{3(c)}(\boldsymbol{l}) = -i\frac{g_1^\theta g_A^3}{8F_\pi^3}\left\{\frac{1}{16\pi^2}\frac{1+\frac{3}{2}\xi}{\sqrt{\xi(1+\xi)}}\ln\left(\frac{\sqrt{1+\xi}+\sqrt{\xi}}{\sqrt{1+\xi}-\sqrt{\xi}}\right) + \left[3L-\frac{3}{2}\frac{1}{16\pi^2}\left(\ln\left(\frac{\mu^2}{M_\pi^2}\right)-1\right)-\frac{1}{16\pi^2}\right]\right\} \times\Big[(\tau^3_{(1)}-\tau^3_{(2)})(\boldsymbol{\sigma}_{(1)}+\boldsymbol{\sigma}_{(2)}) + (\tau^3_{(1)}+\tau^3_{(2)})(\boldsymbol{\sigma}_{(1)}-\boldsymbol{\sigma}_{(2)})\Big]\cdot\boldsymbol{l}\,. \quad (23)$$

Resorting again to the method presented in [58–60] to isolate the irreducible component of the box potential operator fig. 3 (*b*), the latter is found to be the negative of eq. (23) and to cancel the crossed-box-potential operator fig. 3 (*c*). Therefore, contributions to the total CP-violating transition current induced by the CP-violating two-nucleon one-loop potential are absent to $\mathsf{N^2LO}$ —not only in the deuteron channel.

The only non-vanishing $\mathsf{N^2LO}$ contributions are thus the vertex corrections shown in diagrams 3 (*e*) and (*f*). The vertex correction on the CP-conserving vertex is readily accounted for, since we use the physical πNN coupling constant in our calculations. The situation is somewhat different for diagram 3 (*e*), where the physical value of the coupling constant is not known, but was calculated/estimated in sect. 2. Since g_0^θ only appears at the one-loop level in the case of the deuteron EDM, we only need to consider g_1^θ here. The quoted uncertainty for g_1^θ is of the order of 50%. On the other hand, the corresponding correction for the CP-conserving πNN coupling constant, the so-called Goldberger-Treiman discrepancy, is very small [64], such that we may safely assume that the uncertainty given for g_1^θ is sufficiently large such that it includes vertex corrections.

Thus, the only piece of the NN potential that is CP-odd *and* contributes to the deuteron EDM is the tree-level diagram depicted in fig. 3 (*a*), with the g_1^θ coupling employed in the CP-odd πNN vertex: it is the LO potential.

4.2 Contributions from the CP-odd irreducible NN transition current

In order for an irreducible transition current not to vanish in the deuteron channel, it has to induce ${}^3S_1$-${}^3D_1 \to {}^3S_1$-${}^3D_1$ (isospin 0 to isospin 0 and spin 1 to spin 1) transitions. It therefore needs to be an isoscalar operator, symmetric in spin space. Therefore the tree-level transition currents —cf. fig. 5 (*a*)— that are all isovector in character, do not contribute to the deuteron EDM. The relevant CP-odd irreducible one-loop NN current operators are listed in fig. 5 (*b*)–(*j*). Diagrams involving CP-even $NN\pi\gamma$ vertices have been neglected here since, to the order we are working, they do not yield EDM contributions: according to eq. (15) EDM contributions are extracted from the 0th component of matrix elements of transition currents. The leading order, CP-even $NN\pi\gamma$ vertex $ie(g_A/F_\pi)\,\varepsilon\cdot S\epsilon^{a3b}\tau^b$ (see appendix A of [37] where γ is the "Coulomb photon", $\varepsilon=(1,\mathbf{0})$) does not have a non-vanishing 0th component for $S=(0,\boldsymbol{\sigma}/2)$.

The diagram classes depicted in fig. 5 (*g*) and (*h*) are of order $g_0^\theta\, e/(m_N^2 F_\pi)$ and thus $\mathsf{N^2LO}$. For a photon coupling to nucleon 2 the two-nucleon-irreducible component of diagram fig. 5 (*g*) and diagram fig. 5 (*h*) give

$$\left(J^{\theta\,\mathsf{N^2LO}}_{5(g+h)}\right)^\mu = i\frac{e g_0^\theta g_A^3}{128\pi F_\pi^3 M_\pi}\left[\frac{1}{1+\xi}+\frac{2}{\sqrt{\xi}}\arctan\sqrt{\xi}\right]v^\mu \times(\boldsymbol{\tau}_{(1)}\cdot\boldsymbol{\tau}_{(2)}-\tau^3_{(2)})(\boldsymbol{\sigma}_{(1)}-\boldsymbol{\sigma}_{(2)})\cdot(\boldsymbol{p}_2'-\boldsymbol{p}_2+\boldsymbol{q}), \quad (24)$$

with $\xi=|\boldsymbol{p}_2'-\boldsymbol{p}_2+\boldsymbol{q}|^2/(4M_\pi^2)$ in terms of the initial (final) momentum $p_i(p_i')$ of nucleon i and the momentum of the out-going photon q. Although the operator (24) contains an isospin-symmetric component, it is spin-antisymmetric and vanishes in the deuteron channel.

The diagram classes depicted in fig. 5 (*d*) and (*e*) vanish in the deuteron channel, since they are isovectors.

In addition there are diagrams at $\mathsf{N^2LO}$ where the photon couples to a vertex correction (fig. 5 (*i*) and (*j*)); however, terms that contain the g_0^θ vertex turn out to be isovectors and thus do not contribute to the deuteron channel, and those that contain g_1^θ start to contribute only at $\mathsf{N^3LO}$.

The triangular diagrams depicted in fig. 5 (*b*), (*c*) and (*f*) are all of order $\mathsf{N^2LO}$. Diagrams of the types of fig. 5 (*c*) and (*f*) vanish in the deuteron channel which can be readily seen from their isospin components: diagram fig. 5 (*c*) is proportional to $\tau^3_{(2)}$ (photon coupling to nucleon 2) and diagram fig. 5 (*f*) is proportional to $2\tau_{(2)}+i(\boldsymbol{\tau}_{(1)}\times\boldsymbol{\tau}_{(2)})$. A class of currents that has a spin- and isospin-symmetric component is depicted in fig. 5 (*b*),

$$\left(J^{\theta\,\mathsf{N^2LO}}_{5(b)}\right)^\mu = i\frac{e g_0^\theta g_A}{4F_\pi^3}\,v^\mu\,\left(\boldsymbol{\tau}_{(1)}\cdot\boldsymbol{\tau}_{(2)}-\tau^3_{(2)}\right) \times\left(I(p_1-p_1')\,(\boldsymbol{p}_1'-\boldsymbol{p}_1)\cdot\boldsymbol{\sigma}_{(2)}+(1\leftrightarrow 2)\right), \quad (25)$$

with $I(l) = -\arctan(|\boldsymbol{l}\,|/(2M_\pi))/(8\pi|\boldsymbol{l}\,|)$ [37]. Resorting to the CD-Bonn wave function of the deuteron as used above, the resulting g_0^θ contribution to the deuteron EDM for the ${}^3S_1$-state and ${}^3D_1$-admixture is found to be

$$d^\theta_{5(b)} = \underbrace{-2.00\cdot 10^{-4}\times G_\pi^0\, e\,\mathrm{fm}}_{{}^3S_1} - \underbrace{0.53\cdot 10^{-4}\times G_\pi^0\, e\,\mathrm{fm}}_{{}^3D_1\text{-adm.}}, \tag{26}$$

where $G_\pi^0 := g_0^\theta g_A m_N/F_\pi$.

The class of diagrams depicted in fig. 5 (k), see ref. [23], gives

$$\left(J^{\theta\,\mathsf{N^2LO}}_{5(k)}\right)^0 = -i\frac{e g_0^\theta g_A \delta m_{np}}{F_\pi}\left(\boldsymbol{\tau}_{(1)}\cdot\boldsymbol{\tau}_{(2)} - \tau^3_{(1)}\tau^3_{(2)}\right) \times \frac{\boldsymbol{\sigma}_{(1)}\cdot(\boldsymbol{p}_1-\boldsymbol{p}_1') + \boldsymbol{\sigma}_{(2)}\cdot(\boldsymbol{p}_2-\boldsymbol{p}_2')}{[(\boldsymbol{p}_1-\boldsymbol{p}_1')^2+M_\pi^2]\,[(\boldsymbol{p}_2-\boldsymbol{p}_2')^2+M_\pi^2]}\,. \tag{27}$$

The explicit evaluation of the EDM contribution of fig. 5 (k) yields $0.31\cdot 10^{-4}\times G_\pi^0\, e\,\mathrm{fm}$, which justifies the classification as $\mathsf{N^2LO}$.

The absence of *both* —divergences and (undetermined) counterterms up to $\mathsf{N^2LO}$— ensures the predictive power of the two-nucleon contributions to the deuteron EDM that is induced by the θ-term. Together with the g_1^θ contribution the total two-nucleon contribution to the EDM of the deuteron induced by the θ-term is then given by

$$\begin{aligned} d^\theta &= d^\theta_{\mathsf{LO}} + d^\theta_{\mathsf{N^2LO}} \\ &= \left[\left(-15.2\cdot\frac{g_1^\theta}{g_0^\theta} - 0.22\right)\pm 0.03\right]\times 10^{-3}\, G_\pi^0\, e\,\mathrm{fm}, \end{aligned} \tag{28}$$

where the uncertainty estimates the higher-order contributions not included as given by the power counting. Alternatively we may express the result directly in terms of $\bar\theta$, the strength of the QCD θ-term, and write

$$\begin{aligned} d^\theta &= d^\theta_{\mathsf{LO}} + d^\theta_{\mathsf{N^2LO}} \\ &= -\big((5.9\pm 3.9) - (0.5\pm 0.2)\big)\times 10^{-4}\,\bar\theta\, e\,\mathrm{fm}, \end{aligned} \tag{29}$$

where the uncertainties now contain, in addition to the one given in eq. (28), also the uncertainties in the coupling constants g_0^θ and g_1^θ. Therefore the final result is completely dominated by the contribution from the CP- and isospin-violating tree-level potential proportional to g_1^θ.

5 Summary and conclusions

As already stated in the introduction, the established relation between the QCD θ-term and the CP-odd πNN coupling constant is not sufficient to predict the size of the electric dipole moment of a *single* nucleon (neutron or proton) with the help of effective field theory, since the calculable one-loop contributions are of the same order as undetermined counterterms. However, this unpleasant feature is not present for the two-nucleon contributions of the deuteron and other light nuclei, which contribute already at tree-level order —unaffected by any counterterms— and which can be derived —admittedly with a large uncertainty— up-to-and-including the order $\mathsf{N^2LO}$, see eqs. (28) and (29) at the end of sect. 4.2. The $\mathsf{N^2LO}$ contributions of these results are (up to vertex corrections discussed in sect. 3) solely governed by the irreducible transition currents. The latter include loops which for the first time have been calculated in the present work. Note that any contribution with unknown coefficients can only show up at $\mathsf{N^3LO}$.

The dominant part of the deuteron's two-nucleon EDM from the QCD θ-term resulted from an isospin-violating, CP-odd πNN coupling constant, g_1. The isospin violation of this coupling can be estimated from the strong contribution to the pion mass-square splitting $(\delta M_\pi^2)^{\mathrm{str}}/(M_\pi^2\epsilon)$. Although this ratio gives a small number, its contribution to g_1^θ gets enhanced by the relatively large pion-nucleon sigma term. Nominally, g_1^θ should be suppressed by two orders relative to its isospin-conserving counterpart, g_0^θ. However, the latter is governed by the strong part of the neutron-proton mass splitting and therefore is found to be exceptionably small. Thus the isospin-violating coupling g_1^θ —as already observed by Lebedev *et al.* [19]— is effectively only suppressed by one power in the counting.

This is important since the one-pion exchange with one g_0^θ vertex cannot contribute to the two-nucleon part of the deuteron EDM because of isospin selection. This was summarized in the folklore that the deuteron would be blind to the two-nucleon contributions generated by the θ-term. This folklore, however, should be abandoned. A measurement of a non-vanishing neutron, a non-vanishing proton and a non-vanishing deuteron EDM would suffice to determine the strength of the QCD θ-term, $\bar\theta$, from data. In fact, the two-nucleon part of the deuteron EDM given in (29) is of the same magnitude and therefore comparable in size with the non-analytic isovector part of the nucleon EDM as calculated in ref. [33], which is, using as input the value of g_0^θ from eq. (6),

$$d_N^{\text{non-analyt.}} = (21\pm 9)\times 10^{-4}\,\bar\theta\, e\,\mathrm{fm}, \tag{30}$$

where the uncertainty contains both the variation of the loop scale as proposed in ref. [33] as well as the uncertainty in g_0^θ. This number may presumably be taken as a scale which governs the single nucleon EDMs. However, the non-analytic contribution to the isoscalar part of the nucleon EDM is an order of magnitude smaller due to a suppression by a factor M_π/m_N as well as the absence of a chiral logarithm. Whether the proton or neutron EDM are really of the same magnitude as the two-nucleon part of the deuteron EDM is a question which *only* experiments might eventually be able to answer.

Fact is that, under the assumption that the electric dipole moments are driven by the CP violation that is induced by the QCD θ-term, we now can give a relation between the total EDMs of the deuteron, the neutron and

the proton and the calculated two-nucleon EDM part of the deuteron,

$$d_D = d_n + d_p - \big((5.9\pm3.9) - (0.5\pm0.2)\big)\times 10^{-4}\,\bar\theta\, e\,\mathrm{fm}. \quad (31)$$

A cross-check of the so-extracted $\bar\theta$ value would be possible —still solely from data— by a measurement of the EDM of ^{3}He. Another strategy to test or falsify the $\bar\theta$ value would involve lattice QCD calculations and just two successful EDM measurements, namely one single-nucleon EDM, *i.e.* the one of the neutron or proton, and the deuteron EDM. If even all three of them are measured, then one could use lattice QCD for a first test correlating the proton and neutron EDM results in terms of the parameter $\bar\theta$ and to use formula (31) for an additional, orthogonal test.

If indeed the QCD θ-term would have failed these tests —either by a direct comparison of data or by the additional involvement of lattice QCD— then the following picture would emerge: in case $d_D - d_n - d_p$ is sizable *compared to what eq.* (31) *in combination with experimental or lattice data predicts*, then the dimensional analysis reveals a dominance of the quark-color EDM, feeding the coupling proportional to ${g_1}^3$. On the other hand, if this difference is very small, most probably neither the θ-term nor the quark-color EDM is at work, but one or several of the other dimension six CP-violating operators [23,65]. More insight can be gained from a study of the EDM for ^{3}He. This reasoning stresses once more the need for high-precision measurements, not only of the neutron EDM but also of the EDMs for light ions like proton, deuteron and ^{3}He.

We would like to thank W. Bernreuther, E. Epelbaum, F.-K. Guo, J. Haidenbauer, U. van Kolck, B. Kubis, E. Mereghetti, N.N. Nikolaev, J. Pretz, F. Rathmann, R.G.E. Timmermans and J. de Vries for helpful discussions and T. Lähde also for advice on the numerical analysis. This work is supported in part by the DFG and the NSFC through funds provided to the Sino-German CRC 110 "Symmetries and the Emergence of Structure in QCD", and by the European Community-Research Infrastructure Integrating Activity "Study of Strongly Interacting Matter" (acronym HadronPhysics3). The numerical calculations were partly performed on the supercomputer cluster of the JSC, Jülich, Germany.

Appendix A. Selection of the ground state

As pointed out in [4, 66] the presence of a term in the Lagrangian which explicitly breaks the $SU(2) \times SU(2)$ symmetry imposes a constraint on the selection of the ground state, such that the $SU(2)$ subgroup to which $SU(2) \times SU(2)$ is broken is uniquely specified. This implies especially the absence of pion tadpoles. Therefore, the incorporation of CP-violating and chiral-symmetry-breaking terms into the Lagrangian requires, in general, an adjustment of the vacuum, *i.e.* an axial transformation $A(= R = L^\dagger)$,

$$U \mapsto AUA \quad N \mapsto K(A^\dagger, A, U)N, \quad (A.1)$$

with $U = u^2$ (see, *e.g.*, [37]). In the representation which we are using, the θ-term is related to the isospin-breaking mass term by an axial rotation that contains τ_3 only, $A = \exp(i\alpha\tau_3/2)$ —cf. the discussion at the beginning of sect. 2. Since CP violation is a small perturbation, it will slightly shift the ground state $U_0 = \mathbf{1}_2$ according to $U_0 \mapsto AU_0A$. The rotation angle α is determined by minimizing the potential V in the vicinity of the ground state U_0,

$$\partial V[U = AU_0A]/\partial\alpha = 0. \quad (A.2)$$

The term $F_\pi^2\langle\chi_+\rangle/4$ belonging to the second-order Lagrangian in the pion sector (see $\mathcal{L}_1$ in ref. [67]) would, by itself, not induce a vacuum shift (*i.e.* $\alpha(\bar\theta) = 0$), since the pseudoscalar source p in eq. (2) is purely isoscalar. Thus leading-order tadpoles are avoided. However, the l_7 term of the subleading fourth-order Lagrangian in the pion sector, see $\mathcal{L}_2$ and eq. (5.5) in ref. [67], does give rise to a (π_3) tadpole term,

$$-\frac{l_7}{16}\langle\chi_-\rangle^2 = -l_7(1-\epsilon^2)\epsilon M_\pi^4\bar\theta\frac{\pi_3}{F_\pi}\left(1-\frac{2\pi^2}{3F_\pi^2}\right)+\dots\,. \quad (A.3)$$

Therefore, this tadpole contribution has to be canceled by a perturbative shift of the leading-order term $F_\pi^2\langle\chi_+\rangle/4$ that is induced by an axial rotation of the ground state by the small angle

$$\alpha'(\bar\theta) = -l_7(1-\epsilon^2)\epsilon\frac{M_\pi^2}{F_\pi^2}\bar\theta + \mathcal{O}(\bar\theta^2). \quad (A.4)$$

In contradistinction, the $\mathcal{L}_2$-terms proportional to l_1, l_2, l_5, l_6 and to the so-called high-energy constants, see ref. [67], are invariant under the rotation A. Furthermore, the $\mathcal{L}_2$ term proportional to l_4 does not contribute either, since here the sole external current is the electromagnetic field and since $[\chi, Q] = 0$ (Q: quark charge matrix). Thus there remain only higher-order contributions which are generated by the l_3 and l_7 terms of $\mathcal{L}_2$. These contributions scale as the sixth-order terms of the pion-sector Lagrangian, *i.e.* as $\mathcal{L}_3$ in the notation of ref. [67], and can be neglected here.

However, the redefinition of the ground state also induces new structures into the *pion-nucleon* Lagrangian [31], namely

$$c_1\langle\chi_+\rangle N^\dagger N \to -4\alpha'(\bar\theta)c_1M_\pi^2\frac{\pi_3}{F_\pi}\left(1-\frac{\pi^2}{6F_\pi^2}\right)N^\dagger N+\dots,$$
$$c_5N^\dagger\hat\chi_+N \to -2\alpha'(\bar\theta)c_5\epsilon M_\pi^2N^\dagger\left(\frac{\boldsymbol{\pi}\cdot\boldsymbol{\tau}}{F_\pi}-\frac{(1-\epsilon^2)\bar\theta\tau_3}{2\epsilon}\right)N$$
$$+\dots\,. \quad (A.5)$$

The terms proportional to c_2, c_3, c_4, c_6 and c_7 in the pion-nucleon Lagrangian [68] are invariant under the axial

[3] Note that ref. [23] stated the dominance of the quark-color mechanism already under the assumption that $d_D - d_n - d_p$ itself is sizeable. The difference emerges since in ref. [23] the relative suppression between g_1^θ and g_0^θ was taken from naive dimensional analysis that predicts a negligible contribution from the g_1^θ-term.

rotation A when the electromagnetic field is the sole external current. The $c_5\tau_3$ term is proportional to $\mathcal{O}(\bar\theta^2)$ and can be disregarded. While the remaining c_5 term in (A.5) provides a correction to the value of g_0^θ, the term proportional to c_1 is a new structure: a g_1^θ vertex which is driven by the low energy constant l_7. The latter is related to the strong-interaction part of the pion mass-square shift $(\delta M_\pi^2)^{\rm str}$ by [67],

$$\begin{aligned}(\delta M_\pi^2)^{\rm str} &:= \left(M_{\pi^+}^2 - M_{\pi^0}^2\right)\big|_{\rm strong}\\ &= 2(m_u-m_d)^2B^2 l_7/F_\pi^2 + \ldots\\ &\approx (7\,{\rm MeV})^2 \approx 2M_\pi\cdot 0.18\,{\rm MeV}.\end{aligned} \tag{A.6}$$

This leads to eq. (8), *i.e.*

$$g_1^\theta = \frac{2\,c_1\,(\delta M_\pi^2)^{\rm str}\,(1-\epsilon^2)}{F_\pi\,\epsilon}\bar\theta, \tag{A.7}$$

which agrees with the corresponding term in eq. (113) of [31]. Finally, the correction to g_0^θ is given by

$$\delta g_0^\theta = \frac{\delta m_{np}^{\rm str}\,(1-\epsilon^2)}{4F_\pi\,\epsilon}\,\bar\theta\,\frac{(\delta M_\pi^2)^{\rm str}}{M_\pi^2} = g_0^\theta\,\frac{(\delta M_\pi^2)^{\rm str}}{M_\pi^2}\,, \tag{A.8}$$

reproducing the corresponding term in eq. (113) in [31].

Appendix B. An update of the derivation of Lebedev et al. [19]

In addition to the usual parametrization of the θ-term–induced isospin-conserving and CP-violating πNN coupling,

$$g_0^\theta = \frac{m_*\bar\theta}{F_\pi}\langle N|\bar uu - \bar dd|N\rangle, \tag{B.1}$$

the authors of ref. [19] introduced —via the π^0-η mixing[4]— the isospin-breaking counterpart,

$$g_1^\theta = \frac{m_*\bar\theta}{F_\pi}\,\frac{\sqrt{3}(m_d-m_u)}{4(m_s-\hat m)}\,\frac{1}{\sqrt{3}}\langle N|\bar uu+\bar dd-2\bar ss|N\rangle. \tag{B.2}$$

This is an alternative derivation of the vacuum-alignment result (A.7) for g_1^θ, discussed in appendix A, because the l_7 coefficient of the fourth-order Lagrangian effectively summarizes the π^0-η mixing by the quark-mass–dependent shift to the pion-mass-square $(\delta M_\pi^2)^{\rm str}$.

Inserting the strong-interaction contribution to the neutron-proton mass difference $(m_u-m_d)\langle N|\bar uu-\bar dd|N\rangle = \delta m_{np}^{\rm str}$ and utilizing the parameter ϵ as defined at the beginning of sect. 2, we derive (6) again

$$g_0^\theta = \frac{\delta m_{np}^{\rm str}(1-\epsilon^2)}{4F_\pi\epsilon}\,\bar\theta.$$

Similarly, starting now from eq. (B.2), we get

$$g_1^\theta = \frac{-\bar\theta}{8F_\pi}(1-\epsilon^2)\epsilon\frac{M_\pi^2}{M_K^2-M_\pi^2}\,\hat m\langle N|\bar uu+\bar dd-2\bar ss|N\rangle, \tag{B.3}$$

with $M_\pi^2 = 2B\hat m + \mathcal{O}(\mathcal{M}^2)$ and $M_K^2 = B(m_s+\hat m)+\mathcal{O}(\mathcal{M}^2)$ for the square of the pion and kaon mass, respectively, where here $\mathcal{M}$ is the quark mass matrix for three light flavors. According to refs. [40,69] we have $\hat m\langle N|\bar uu+\bar dd-2\bar ss|N\rangle = \hat m\langle N|\bar uu+\bar dd|N\rangle(1-y)$ with $\sigma_{\pi N}\equiv\sigma_{\pi N}(0) = \hat m\langle p|\bar uu+\bar dd|p\rangle$ and $y\equiv 2\langle p|\bar ss|p\rangle/\langle p|\bar uu+\bar dd|p\rangle$, where $|p\rangle$ denotes here the proton state. The final result is therefore

$$g_1^\theta = -\frac{\bar\theta}{8F_\pi}\,(1-\epsilon^2)\,\epsilon\,\frac{M_\pi^2}{M_K^2-M_\pi^2}\,\sigma_{\pi N}(1-y). \tag{B.4}$$

Inserting $\delta m_{np}^{\rm str} = (2.6\pm0.5)\,{\rm MeV}$ from ref. [41], $F_\pi = 92.2\,{\rm MeV}$, and the $\overline{MS}$ quark masses at 2 GeV from [36], we get

$$g_0^\theta \approx (-0.018\pm0.007)\,\bar\theta \tag{B.5}$$

and

$$g_1^\theta \approx (0.0012\pm0.0004)\,\bar\theta, \tag{B.6}$$

with $\sigma_{\pi N}(0) = 45\,{\rm MeV}$ and $y = 0.21\pm0.20$ from [69] as additional input.

Thus we find

$$\frac{g_1^\theta}{g_0^\theta} = -\frac{\epsilon^2}{2}\,\frac{M_\pi^2}{M_K^2-M_\pi^2}\,\frac{\sigma_{\pi N}(0)(1-y)}{\delta m_{np}^{\rm str}} \approx -0.07\pm0.04, \tag{B.7}$$

as the ratio of the isospin-breaking *versus* the isospin-conserving CP-violating πNN coupling constants which are induced by the θ-term. If we rather applied the values $\sigma_{\pi N}(0) = 59(7)\,{\rm MeV}$ and $y\approx 0$ from refs. [70,71] (for an update of this work see ref. [72]), we would get

$$g_1^\theta \approx (0.0021\pm0.0004)\,\bar\theta \quad\text{and}\quad \frac{g_1^\theta}{g_0^\theta}\approx -0.11\pm0.05, \tag{B.8}$$

as values for g_1^θ and the ratio instead. In summary, the ratios listed in (B.7) and (B.8) are compatible with the estimate (13).

Appendix C. Derivation via SU(3) chiral perturbation theory

In $SU(3)$ ChPT the D-type and F-type CP-violating π^0NN coupling constants are (see, *e.g.*, the $U(3)$ ChPT calculation of ref. [34])

$$g^D_{\pi^0NN} = \frac{4B\bar\theta m_*}{F_\pi}b_D \qquad\text{and}\qquad g^F_{\pi^0NN} = \frac{4B\bar\theta m_*}{F_\pi}b_F,$$

respectively, whereas

$$g^D_{\eta NN} = \frac{-4B\bar\theta m_*}{F_\pi}\,\frac{b_D}{\sqrt{3}} \qquad\text{and}\qquad g^F_{\eta NN} = \frac{4B\bar\theta m_*}{F_\pi}\sqrt{3}b_F$$

[4] Actually, via the π^0-η_8 mixing. For consistency, we replaced here their π^0-η mixing angle by the customary one of chiral perturbation theory [50] —note the explicit $\hat m$ subtraction in the denominator.

Table 3. The value of g_0^θ, g_1^θ, and the ratio g_1^θ/g_0^θ predicted from eqs. (C.1) and (C.2) with i) the original $SU(3)$ parameters b_D and b_F of ref. [37], with ii) the alternative set of parameters based on eqs. (C.5) and (C.6), iii) in the case that $b_D + b_F$ of i) are replaced by c_5 of eq. (C.4). The listed uncertainties do not contain systematical $SU(3)$ errors.

		g_0^θ $[\bar\theta]$	g_1^θ $[\bar\theta]$	g_1^θ/g_0^θ
i)	b_D & b_F from [37]	-0.026 ± 0.002	0.00092 ± 0.00017	-0.036 ± 0.007
ii)	b_D & b_F alternative	-0.023 ± 0.005	0.00088 ± 0.00016	-0.038 ± 0.011
iii)	$b_D + b_F \to c_5$	-0.018 ± 0.007	0.00092 ± 0.00017	-0.051 ± 0.022

are the corresponding ηNN (actually $\eta_8 NN$) counterparts. Here $4B\,b_D$ and $4B\,b_F$ are the coefficients of the anticommutator (D-type) and commutator (F-type) term of the quark mass matrix with the baryon matrix. Therefore, the $SU(3)$ counterparts of eqs. (6) and (B.4) are[5]

$$g_0^\theta = \frac{4B\bar\theta m_*(b_D+b_F)}{F_\pi} = \bar\theta\frac{M_\pi^2}{F_\pi}(1-\epsilon^2)(b_D+b_F), \quad \text{(C.1)}$$

$$g_1^\theta = \frac{4B\bar\theta m_*}{F_\pi}\frac{3b_F-b_D}{\sqrt{3}}\frac{\sqrt{3}}{4}\frac{m_d-m_u}{m_s-\hat m} = \bar\theta\frac{M_\pi^2}{F_\pi}(1-\epsilon^2)(3b_F-b_D)\frac{\epsilon M_\pi^2}{4(M_K^2-M_\pi^2)}\,, \quad \text{(C.2)}$$

where $(\sqrt{3}/4)(m_d-m_u)/(m_s-\hat m)$ is the π^0-η (actually π^0-η_8) mixing angle. Thus, in this case we get the ratio

$$\frac{g_1^\theta}{g_0^\theta} = \frac{\epsilon M_\pi^2}{4(M_K^2-M_\pi^2)}\frac{3b_F-b_D}{b_D+b_F}\,. \quad \text{(C.3)}$$

If the values $b_F = -0.209\,\mathrm{GeV}^{-1}$ and $b_D = 0.066\,\mathrm{GeV}^{-1}$ of ref. [37] are inserted, we get the first row of table 3. However, there is a mismatch by a factor 1.5 approximately between the $SU(3)$ octet quantity,

$$b_D + b_F = -\frac{m_\Xi - m_\Sigma}{4(M_K^2-M_\pi^2)} \approx (-0.143 \pm 0.004)\,\mathrm{GeV}^{-1},$$

used in [5, 32, 33] and the $SU(2)$ low-energy coefficient (LEC),

$$c_5 = \frac{\delta m_{np}^{\mathrm{str}}}{4M_\pi^2\epsilon} \approx (-0.097 \pm 0.034)\,\mathrm{GeV}^{-1}, \quad \text{(C.4)}$$

although according to $SU(3)$ ChPT both quantities should agree to leading order, see eq. (27) of ref. [73][6].

[5] The proportionality of g_1^θ to $3b_F - b_D$ may come at first sight as a surprise. The strange-quark content of the nucleon, however, is proportional to $b_0 + b_D - b_F$ to leading order in the chiral expansion, such that g_1^θ for small or vanishing y is factually proportional to $2b_0 + b_D + b_F$ which in turn is proportional to $2c_1$. For more details see, *e.g.*, refs. [73, 74].

[6] In fact, the latter equation which is based on eq. (5.7) of ref. [74] predicts that the NLO correction to c_5 is much larger than c_5 (or $b_D + b_F$) itself, namely $\Delta c_5 = 0.49\,\mathrm{GeV}^{-1}$. This quantity is of similar size as $\Delta c_1 = +0.2\,\mathrm{GeV}^{-1}$.

Moreover, an alternative procedure to parametrize the above sum is

$$b_D + b_F = \frac{\delta m_{np}^{\mathrm{str}}}{4(M_{K^+}^2 - (M_{\pi^+}^2 - M_{\pi^0}^2) - M_{K^0}^2)} \approx (-0.126 \pm 0.024)\,\mathrm{GeV}^{-1}, \quad \text{(C.5)}$$

where the electromagnetic mass shifts are removed (via the Dashen theorem [75] in the denominator) and where the prediction falls in-between the original one and the c_5 value. Using an analogous parametrization for b_F, we get

$$b_F = \frac{m_{\Sigma^-} - m_{\Sigma^+}}{8(M_{K^+}^2 - (M_{\pi^+}^2 - M_{\pi^0}^2) - M_{K^0}^2)} \approx -0.196\,\mathrm{GeV}^{-1} \quad \text{(C.6)}$$

and $b_D = +(0.069 \pm 0.024)\,\mathrm{GeV}^{-1}$ from (C.5) instead of the above listed values from [37], such that the values in the second row of table 3 are generated instead. The result for $3b_F - b_D$ is approximately the same in both parametrizations, namely $-0.69\,\mathrm{GeV}^{-1}$ in the original one [37] and $-0.66\,\mathrm{GeV}^{-1}$ in the modified one.

Finally, replacing $b_D + b_F$ of [37] by c_5 of eq. (C.4), we get the values in the third row of table 3.

Only the last $SU(3)$ value of the ratio g_1^θ/g_0^θ is in the range of our estimate (13), but all three are compatible with the estimate of (B.7). The quoted numbers of table 3, however, do not contain a systematical error connected with an $SU(3)$ ChPT calculation. For standard quantities such an uncertainty is certainly of the order of 50%. For the quantity c_5 this uncertainty should be rather 100%–200%, see *e.g.* footnote[6]. Taking these $SU(3)$ errors into account, the estimates of table 3 are compatible with the range quoted in (13).

Appendix D. The contribution of the odd-parity nucleon resonance to g_1^θ

According to ref. [36] the mass, width and $N\eta$ branching ratio of the $S_{11}(1535)$ odd-parity nucleon-resonance are $m_{N_{1535}} = (1535 \pm 10)\,\mathrm{MeV}$, $\Gamma_{N_{1535}} = (150 \pm 25)\,\mathrm{MeV}$ and $\mathcal{B}_{N_{1535}\to N\eta} = (42 \pm 10)\%$. Finally the CM momentum is $p^\star = 186\,\mathrm{MeV}$. The partial decay width $\Gamma_{N_{1535}\to N\eta}$ is then approximately 63 MeV, such that one finds for the effective coupling constant for the decay $N^* \to N\eta$

$$|g^\star| = \sqrt{\frac{8\pi\Gamma_{N_{1535}\to N\eta}}{p^\star}} \approx 2.9, \quad \text{(D.1)}$$

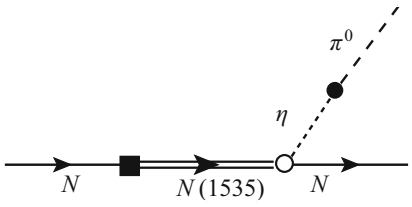

Fig. 6. Effective CP-violating and isospin-violating $\pi_3 NN$ vertex estimated as CP-violating transition (black square) from the even-parity nucleon to the odd-parity $S_{11}(1535)$ nucleon-resonance (double line) which in turn decays into ηN (open circle) with subsequent isospin-breaking by $\eta - \pi^0$ mixing (black circle). The second topology of the diagram, where the pion emission comes first, is included in the calculation.

where we assumed an energy-independent decay vertex. By inserting

$$\frac{1}{2}\langle i\chi_- \rangle = -M_\pi^2(1-\epsilon^2)\bar{\theta}\left(1-\frac{1}{2}\pi^2/F_\pi^2\right)+\epsilon 2M_\pi^2\pi_3/F_\pi+\dots \tag{D.2}$$

into the effective interaction Lagrangian

$$\mathcal{L}_{N_{1535}N} = \tilde{h}N_{1535}^\dagger\frac{1}{2}\langle i\chi_-\rangle N + \text{h.c.}, \tag{D.3}$$

we get

$$\mathcal{L}_{N_{1535}N} = \tilde{h}N_{1535}^\dagger\Big(-M_\pi^2(1-\epsilon^2)\bar{\theta}+\epsilon\frac{2M_\pi^2}{F_\pi}\pi_3 + \dots\Big)N + \text{h.c.} \tag{D.4}$$

The first term provides the CP-odd transition of a nucleon into the N^*. As illustrated in fig. 6, we may model the second vertex by the decay of the resonance into an η and a nucleon, followed by η-π^0 mixing; using the leading-order ChPT expression for the mixing amplitude

$$\epsilon_{\pi^0\eta} \approx \sqrt{\frac{1}{3}}\frac{B(m_d-m_u)}{M_\eta^2-M_\pi^2} \approx 1.37\%, \tag{D.5}$$

we can express $\tilde{h}$ by g^* and $\epsilon_{\pi^0\eta}$ as

$$\tilde{h} = \epsilon_{\pi^0\eta}\frac{F_\pi g^\star}{2\epsilon M_\pi^2}\,. \tag{D.6}$$

Thus the interaction Lagragian (D.4) can be rewritten as

$$\mathcal{L}_{N^\star N\chi_-} = g^\star\epsilon_{\pi^0\eta}\left(\frac{F_\pi(1-\epsilon^2)\bar{\theta}}{-2\epsilon}+\pi_3\right)N_{1535}^* N + \text{h.c.} \tag{D.7}$$

In summary, we get the following estimate for the odd-parity contribution to the CP-violating isospin-breaking πNN coupling constant:

$$\delta g_1^\theta = |g^\star|^2(\epsilon_{\pi^0\tilde{\eta}})^2\frac{\bar{\theta}F_\pi(1-\epsilon^2)/(-\epsilon)}{m_{N_{1535}}-m_N} \approx (0.6\pm 0.3)\cdot 10^{-3}\,\bar{\theta}, \tag{D.8}$$

which is only one third of the NDA estimate

$$|\epsilon|\frac{M_\pi^4}{m_N^3 F_\pi}\,\bar{\theta} \sim 1.7\cdot 10^{-3}\,\bar{\theta}.$$

References

1. I.B. Khriplovich, S.K. Lamoreaux, *CP Violation Without Strangeness: Electric Dipole Moments of Particles, Atoms, and Molecules* (Springer, Berlin, Germany, 1997).
2. I.I.Y. Bigi, A.I. Sanda, *CP Violation*, 2nd edition (Cambridge University Press, Cambridge, UK, 2009).
3. M. Pospelov, A. Ritz, Ann. Phys. **318**, 119 (2005) hep-ph/0504231.
4. V. Baluni, Phys. Rev. D **19**, 2227 (1979).
5. R.J. Crewther, P. Di Vecchia, G. Veneziano, E. Witten, Phys. Lett. B **88**, 123 (1979) **91**, 487(E) (1980).
6. G. 't Hooft, Phys. Rev. Lett. **37**, 8 (1976).
7. W. Buchmüller, D. Wyler, Nucl. Phys. B **268**, 621 (1986).
8. A. De Rujula, M.B. Gavela, O. Pene, F.J. Vegas, Nucl. Phys. B **357**, 311 (1991).
9. B. Grzadkowski, M. Iskrzynski, M. Misiak, J. Rosiek, JHEP **10**, 085 (2010) arXiv:1008.4884 [hep-ph].
10. C.M. Maekawa, E. Mereghetti, J. de Vries, U. van Kolck, Nucl. Phys. A **872**, 117 (2011).
11. J. de Vries, E. Mereghetti, R.G.E. Timmermans, U. van Kolck, arXiv:1212.0990 [hep-ph].
12. M.J. Ramsey-Musolf, S. Su, Phys. Rep. **456**, 1 (2008) hep-ph/0612057.
13. S. Weinberg, Phys. Rev. Lett. **63**, 2333 (1989).
14. T. Mannel, N. Uraltsev, Phys. Rev. D **85**, 096002 (2012) arXiv:1202.6270 [hep-ph].
15. T. Mannel, N. Uraltsev, arXiv:1205.0233 [hep-ph].
16. LHCb Collaboration (R. Aaij *et al.*), Phys. Rev. Lett. **108**, 111602 (2012) arXiv:1112.0938 [hep-ex].
17. CDF Collaboration (T. Aaltonen *et al.*), Phys. Rev. D **85**, 012009 (2012) arXiv:1111.5023 [hep-ex].
18. I.B. Khriplovich, R.A. Korkin, Nucl. Phys. A **665**, 365 (2000) nucl-th/9904081.
19. O. Lebedev, K.A. Olive, M. Pospelov, A. Ritz, Phys. Rev. D **70**, 016003 (2004) hep-ph/0402023.
20. C.-P. Liu, R.G.E. Timmermans, Phys. Rev. C **70**, 055501 (2004) nucl-th/0408060.
21. I. Stetcu, C.-P. Liu, J.L. Friar, A.C. Hayes, P. Navratil, Phys. Lett. B **665**, 168 (2008) arXiv:0804.3815 [nucl-th].
22. J. de Vries, E. Mereghetti, R.G.E. Timmermans, U. van Kolck, Phys. Rev. Lett. **107**, 091804 (2011) arXiv:1102.4068 [hep-ph].
23. J. de Vries, R. Higa, C.-P. Liu, E. Mereghetti, I. Stetcu, R.G.E. Timmermans, U. van Kolck, Phys. Rev. C **84**, 065501 (2011) arXiv:1109.3604 [hep-ph].
24. I.R. Afnan, B.F. Gibson, Phys. Rev. C **82**, 064002 (2010) arXiv:1011.4968 [nucl-th].
25. B.F. Gibson, I.R. Afnan, AIP Conf. Proc. **1441**, 579 (2012).
26. EDM Collaboration (Y.K. Semertzidis *et al.*), AIP Conf. Proc. **698**, 200 (2004) hep-ex/0308063.
27. Y.F. Orlov, W.M. Morse, Y.K. Semertzidis, Phys. Rev. Lett. **96**, 214802 (2006) hep-ex/0605022.
28. D. Anastassopoulos *et al.*, AGS Proposal, April 2008, available from `http://www.bnl.gov/edm/`.
29. A. Lehrach, B. Lorentz, W. Morse, N.N. Nikolaev, F. Rathmann, arXiv:1201.5773 [hep-ex].
30. JEDI Collaboration (R. Engels *et al.*), COSY proposal #216, May 2012, available from `http://collaborations.fz-juelich.de/ikp/jedi/documents/proposals.shtml`.
31. E. Mereghetti, W.H. Hockings, U. van Kolck, Ann. Phys. **325**, 2363 (2010) arXiv:1002.2391 [hep-ph].

32. A. Pich, E. de Rafael, Nucl. Phys. B **367**, 313 (1991).
33. K. Ottnad, B. Kubis, U.-G. Meißner, F.-K. Guo, Phys. Lett. B **687**, 42 (2010) arXiv:0911.3981 [hep-ph].
34. K. Ottnad, Diplom thesis, University of Bonn (2009) unpublished.
35. F.-K. Guo, U.-G. Meißner, JHEP **12**, 097 (2012) arXiv:1210.5887 [hep-ph].
36. Particle Data Group (J. Beringer *et al.*), Phys. Rev. D **86**, 010001 (2012).
37. V. Bernard, N. Kaiser, U.-G. Meißner, Int. J. Mod. Phys. E **4**, 193 (1995) hep-ph/9501384.
38. M. Cini, E. Ferrair, R. Gatto, Phys. Rev. Lett. **2**, 7 (1959).
39. W. Cottingham, Ann. Phys. **25**, 424 (1963).
40. J. Gasser, H. Leutwyler, Phys. Rep. **87**, 77 (1982).
41. A. Walker-Loud, C.E. Carlson, G.A. Miller, Phys. Rev. Lett. **108**, 232301 (2012) arXiv:1203.0254 [nucl-th].
42. S.R. Beane, K. Orginos, M.J. Savage, Nucl. Phys. B **768**, 38 (2007).
43. A. Filin *et al.*, Phys. Lett. B **681**, 423 (2009) arXiv:0907.4671 [nucl-th].
44. E. Mereghetti, J. de Vries, W.H. Hockings, C.M. Maekawa, U. van Kolck, Phys. Lett. B **696**, 97 (2011) arXiv:1010.4078 [hep-ph].
45. V. Baru, C. Hanhart, M. Hoferichter, B. Kubis, A. Nogga, D.R. Phillips, Nucl. Phys. A **872**, 69 (2011) arXiv:1107.5509 [nucl-th].
46. T. Becher, H. Leutwyler, JHEP **06**, 017 (2001) arXiv:hep-ph/0103263.
47. J. Gasser, M.A. Ivanov, E. Lipartia, M. Mojžiš, A. Rusetsky, Eur. Phys. J. C **26**, 13 (2002) arXiv:hep-ph/0206068.
48. P. Büttiker, U.-G. Meißner, Nucl. Phys. A **668**, 97 (2000) arXiv:hep-ph/9908247.
49. N. Fettes, U.-G. Meißner, Nucl. Phys. A **676**, 311 (2000) arXiv:hep-ph/0002162.
50. J. Gasser, H. Leutwyler, Nucl. Phys. B **250**, 539 (1985).
51. A.M. Gasparyan, J. Haidenbauer, C. Hanhart, J. Speth, Phys. Rev. C **68**, 045207 (2003) nucl-th/0307072.
52. S. Weinberg, Phys. Lett. B **295**, 114 (1992) hep-ph/9209257.
53. S. Liebig *et al.*, Eur. Phys. J. A **47**, 69 (2011) arXiv:1003.3826 [nucl-th].
54. V. Baru, C. Hanhart, A. Nogga, in preparation.
55. U. van Kolck, M.C.M. Rentmeester, J.L. Friar, J.T. Goldman, J.J. de Swart, Phys. Rev. Lett. **80**, 4386 (1998) nucl-th/9710067.
56. R. Machleidt, Phys. Rev. C **63**, 024001 (2001) nucl-th/0006014.
57. J. Haidenbauer, W. Plessas, Phys. Rev. C **30**, 1822 (1984).
58. N. Kaiser, R. Brockmann, W. Weise, Nucl. Phys. A **625**, 758 (1997) nucl-th/9706045.
59. N. Kaiser, Phys. Rev. C **62**, 024001 (2000) nucl-th/9912054.
60. S.-L. Zhu, C.M. Maekawa, B.R. Holstein, M.J. Ramsey-Musolf, U. van Kolck, Nucl. Phys. A **748**, 435 (2005) nucl-th/0407087.
61. R.B. Wiringa, V.G.J. Stoks, R. Schiavilla, Phys. Rev. C **51**, 38 (1995) nucl-th/9408016.
62. V.G.J. Stoks, R.A.M. Klomp, C.P.F. Terheggen, J.J. de Swart, Phys. Rev. C **49**, 2950 (1994) nucl-th/9406039.
63. R. Timmermans, private communication.
64. V. Bernard, Prog. Part. Nucl. Phys. **60**, 82 (2008) arXiv:0706.0312 [hep-ph].
65. J. de Vries, R.G.E. Timmermans, E. Mereghetti, U. van Kolck, Phys. Lett. B **695**, 268 (2011) arXiv:1006.2304 [hep-ph].
66. R.F. Dashen, Phys. Rev. D **3**, 1879 (1971).
67. J. Gasser, H. Leutwyler, Ann. Phys. **158**, 142 (1984).
68. N. Fettes, U.-G. Meißner, S. Steininger, Nucl. Phys. A **640**, 199 (1998) hep-ph/9803266.
69. B. Borasoy, U.-G. Meißner, Ann. Phys. **254**, 192 (1997) hep-ph/9607432.
70. J.M. Alarcon, J. Martin Camalich, J.A. Oller, Phys. Rev. D **85**, 051503 (2012) arXiv:1110.3797 [hep-ph].
71. J. Martin Camalich, J.M. Alarcon, J.A. Oller, Prog. Part. Nucl. Phys. **67**, 327 (2012) arXiv:1111.4934 [hep-ph].
72. J.M. Alarcon, L.S. Geng, J.M. Camalich, J.A. Oller, arXiv:1209.2870 [hep-ph].
73. M. Mai, P.C. Bruns, B. Kubis, U.-G. Meißner, Phys. Rev. D **80**, 094006 (2009) arXiv:0905.2810 [hep-ph].
74. M. Frink, U.-G. Meißner, JHEP **07**, 028 (2004) hep-lat/0404018.
75. R.F. Dashen, Phys. Rev. **183**, 1245 (1969).